STATUS OF THE NOAA/NESDIS OPERATIONAL SATELLITE WIND PRODUCT SYSTEM: RECENT IMPROVEMENTS, NEW PRODUCTS, PRODUCT QUALITY, AND FUTURE PLANS

Jaime Daniels[1], Christopher Velden[2], Wayne Bresky[3], and Antonio Irving[4]

[1] NOAA/NESDIS, Office of Research and Applications, Camp Springs, Maryland 20746
[2] Cooperative Institute for Meteorological Satellite Studies (CIMSS), Madison, Wisconsin
[3] Raytheon Information Technology and Scientific Services Lanham, Maryland 20706
[4] NOAA/NESDIS, Office of Satellite Data Processing and Distribution Camp Springs, Maryland 20746

ABSTRACT

This paper provides a summary of the status of the NOAA/NESDIS operational satellite wind product system. Recent improvements, new additions, future plans and product quality assessment of the Atmospheric Motion Vector (AMV) product suite will be discussed. GOES-10 still serves as the western operational geostationary satellite and GOES-9 has been activated to provide coverage over the western Pacific for the International community until MTSAT-1R is launched and readied for operational service. On April 1, 2003, GOES-12 replaced GOES-8 as the eastern operational geostationary satellite. The inclusion of a 13.3µm channel on the GOES-12 imager has led to better height estimates of cloud tracers and has therefore improved the overall quality of the GOES-12 cloud drift wind products. Validation results for the GOES-12 AMVs will be shown, along with a synopsis of our early experiences with the utilization of these products in operational Numerical Weather Prediction (NWP) systems based on feedback from the ECMWF and UKMET. The 3.9µm cloud drift wind product has now been transitioned into the operational environment at NOAA/NESDIS providing improved low-level cloud drift wind coverage at night in both the large scale and storm scale environments. These products are being made available for use in NWP assimilation systems and for use by National Weather Service (NWS) field forecasters. For the first time, AMVs derived from measurements taken from a polar orbiting satellite, are being planned to be transitioned into the operational NOAA/NESDIS AMV product suite. AMVs are currently being derived from the Moderate Resolution Imaging Spectroradiometer (MODIS) instrument aboard the National Aeronautical and Space Administration (NASA) polar orbiting Terra and Aqua satellites on an experimental basis at NOAA/NESDIS. MODIS AMVs are being routinely validated against radiosonde wind observations and NCEP/GFS wind analyses; these results will be discussed. Operational transition plans, which include product dissemination, will also be discussed.

1. INTRODUCTION

The NOAA/NESDIS winds processing system continues to be incrementally upgraded with updated wind algorithms, new wind products, and new processing strategies. Section 2 provides the status of the GOES satellites, current and new operational wind products, product quality monitoring statistics and dissemination plans for these products. In addition, a brief description of the transition experience involving GOES-12 and the plans to transition the Moderate Resolution Imaging Spectroradiometer (MODIS) winds processing capability into NESDIS operation is discussed in this section. Section 3 is dedicated to the issue of height assignment. GOES-12 AMV height assignments derived from the CO2 slicing are presented in this section. Results from a best-fit analysis of AMVs are also presented in this section in an attempt to characterize the errors associated with the heights assigned to these AMVs. Section 4 describes NOAA/NESDIS' and CIMSS' participation in field experiments where cloud-drift winds were derived from rapid scan imagery.

2. NESDIS OPERATIONS STATUS REPORT

2.1 Status of GOES satellites

NOAA/NESDIS currently maintains a continuous stream of data from three geostationary environmental operational satellites. At the present time, these three operational satellites include GOES-12 at 75°W, GOES-10 at 135°W, and GOES-9 at 155°E. The GOES-12 satellite, which was launched on July 23, 2001, officially replaced GOES-8 as the eastern operational geostationary satellite on May 1, 2003. Per an agreement between the National Oceanic and Atmospheric Administration (NOAA) and the Japan Meteorological Agency (JMA), the GOES-9 satellite became the operational geostationary satellite at 155°E on May 22, 2003 ensuring continuous earth observations over the western Pacific Ocean. The GOES-11 satellite remains a fully capable on-orbit spare. GOES-11 carries the same instrumentation as the previous three in the GOES-I/M satellites. Current plans call for the launch of the GOES-N satellite in December 2004 with a full checkout of the system to occur in the Spring of 2005. GOES-N carries the same instrumentation as GOES-12.

2.2 Operational wind products, dissemination, and product monitoring

The current operational wind products being generated at NOAA/NESDIS are shown in Table 1. The frequency at which each product is produced, together with the GOES image sector used, and image interval is presented in this table. All of the operational NESDIS wind products shown in Table 1 are encoded into the unified BUFR format and available on a NESDIS server. All of the products, with the exception of the sounder water vapor winds, will continue to be encoded into the SATOB format and distributed over the Global Telecommunication System (GTS).

Wind Product	*Frequency (Hours)*	*Image Sector(s)*	*Image Interval (minutes)*
IR Cloud-drift (11um)	3	RISOP	7.5
	3	CONUS/PACUS	15
	3	Extended NH: SH	30
IR Cloud-drift (3.9um)	3	RISOP	7.5
	3	CONUS/PACUS	15
		Extended NH: SH	30
Water Vapor	3	Extended NH; SH	30
Visible Cloud-drift	3	RISOP	7.5
	3	PACU/CONUS	15
	3	Extended NH; SH	30
Sounder WV (7.4um)	3,6	CONUS/Tropical	60
Sounder WV (7.0um)	3,6	CONUS/Tropical	60

Table 1. NOAA/NESDIS operational satellite wind products

The newest operational AMV product is the low-level cloud-drift wind product generated from the 3.9µm channel (Dunion and Velden 2002a). This is a night-time, low level wind product that will complement the day-time, low-level visible cloud-drift wind product. Preparations are being made to distribute this new product over the National Weather Services Advanced Weather Interactive Processing System (AWIPS) giving NWS field forecasters access to this new product. Further preparations are being made to distribute this new AMV product over the Global Telecommunication System (GTS). Operational distribution over AWIPS and the GTS are expected to begin in the Fall 2004.

In the near future, we will begin testing the generation of AMVs on an hourly basis instead of a three hourly basis. It is anticipated that more continuous AMV observations will help improve the accuracy of Numerical Weather Prediction (NWP) model forecasts and aid forecasters in the field. LeMarshall et al. 2002, for example, demonstrated that improvements in regional model forecasts over Australia could be gained when hourly IR and visible AMVs were assimilated. Forecast impact tests involving these hourly AMV products will be planned through the Joint Center for Satellite Data Assimilation (JCSDA).

Like other satellite producers, NOAA/NESDIS continue to rely on collocated AMVs and rawinsonde observations to assess and monitor the quality the AMVs. Time series of verification statistics can be found at: http://www.orbit.nesdis.noaa.gov/smcd/opdb/goes/winds/html/tseries.html. A five year time series of daily verification statistics (sat-rawinsonde mean vector difference and wind speed bias) for upper level (100-400mb) GOES-East and GOES-West IR cloud drift winds are shown in Figures 1a and 1b. A steady reduction in the magnitudes of the AMV error statistics is observed in these time series. These improvements are reflective of the implementation of numerous advances made to the operational AMV production suite. The observed trends in improved accuracy are generally reflective of trends observed at other global AMV processing centers.

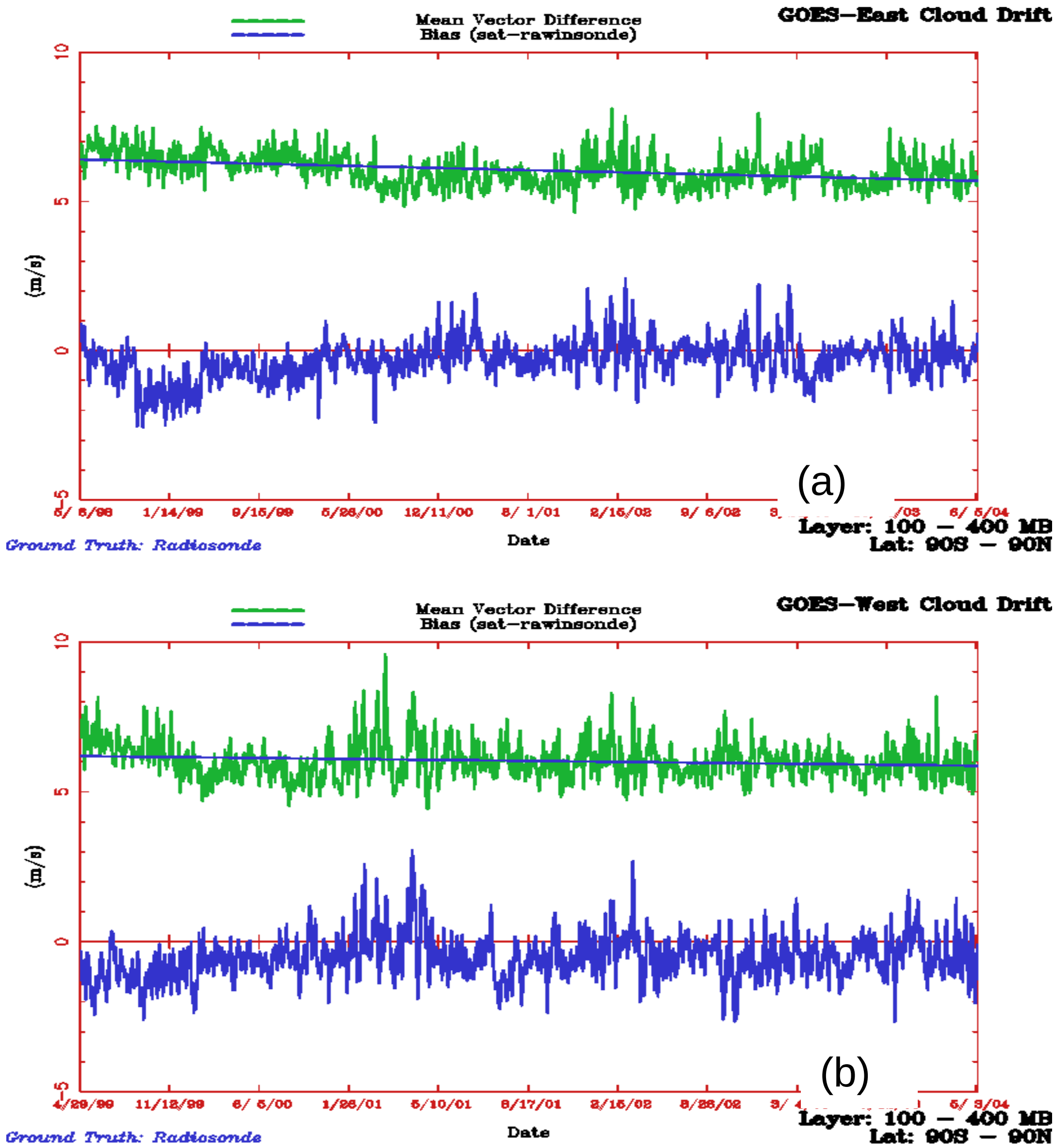

Figure 1. Mean vector difference and speed bias (sat-rawinsonde) for GOES-E (a) and GOES-W (b) upper level (100-400mb) IR cloud-drift winds.

2.3 Quality assessment of GOES-12 AMVs

On May 1, 2003, the GOES-12 satellite officially replaced GOES-8 as the eastern operational geostationary satellite. Changes made to the GOES-12 imager instrument include the addition of a 13.3µm channel and a higher resolution (4km) water vapor channel. The addition of the 13.3µm channel allowed, for the first time since GOES-7, the use of the well-known CO_2 slicing algorithm (Menzel, et al, 1983) to assign heights to viable cloud tracers. The resultant CO_2 slicing algorithm height assignments will supplement the height assignments provided by the water vapor intercept algorithm (Szejwach, 1982).

The European Center for Medium Range Weather Forecasting (ECMWF) and the United Kingdom (UK) Meteorological Office routinely received GOES-12 winds from NESDIS and provided feedback regarding their quality as measured by comparisons to their respective model background and assimilation wind fields. ECMWF experiments showed that the GOES-12 high level (100-400hPa) cloud-drift winds exhibited a strong slow speed bias in the Northern Hemisphere extra-tropics. This can be seen in Figure 2 which shows a density plot of GOES-12 high level cloud drift wind speeds (y-axis) versus wind speeds from the ECMWF model background (x-axis) over the period 4/7/2003 (18Z)–4/14/2003 (00Z). The density plot for the corresponding GOES-8 high level cloud drift wind speeds versus the ECMWF model background over the same period is also shown in this figure. Note how symmetric the density plot is for GOES-8 where the mean speed difference is 0.29m/s. For GOES-12, note the skewness in the density plot where the mean speed difference is -0.65 m/s.

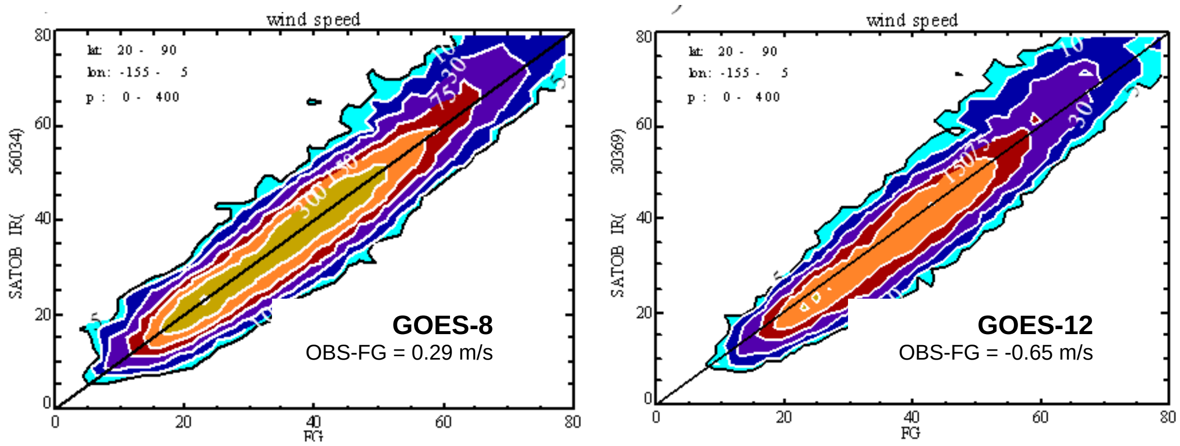

Figure 2. Speed density plots showing observed IR high level (100-400mb) wind speeds against ECMWF model background wind speeds for GOES-8 (left) and GOES-12 (right) for 7-14, April 2003. (Courtesy of Lueder Von Bremen, ECMWF)

Our evaluation of GOES-12 cloud-drift winds quality, as measured against rawinsondes over the CONtinental United States (CONUS) during the period 4/25–4/30/2003 also revealed the existence of a significant slow speed bias. These statistics are shown in Table 2 and include GOES-12 winds whose height assignments are computed using the CO_2 Slicing (Menzel, et al, 1983), water vapor intercept (Szejwach, 1982), and the infrared window height algorithms.

Statistic	**Satellite Wind**	**GFS model guess**	**Raob**
Mean Vector Difference (m/s)	6.86	6.22	
Sat-Raob Speed Bias (m/s)	-1.84	-1.27	
Speed	24.87	25.42	26.69
Sample Size	3220	3220	3220

Table 2. Comparison statistics between collocated GOES-12 High Level (100-400mb) IR cloud-drift winds and rawinsondes over CONUS for the period April 25-30, 2003. CO2 heights, H2O-intercept heights, and window heights are included in this sample.

Similar statistics were generated again, but the sample was stratified by height assignment method. Tables 3 and 4 show these statistics for the GOES-12 cloud drift winds whose height assignments were computed from the CO_2-IRW ratio algorithm and the water vapor intercept algorithm, respectively. Both sets of statistics indicate the presence of a significant slow bias for both height methods, with the magnitude of the slow speed bias being larger for the winds assigned the CO_2 heights.

Statistic	Satellite Wind	GFS model guess	Raob
Mean Vector Difference (m/s)	6.82	6.28	
Sat-Raob Speed Bias (m/s)	-1.93	-1.24	
Speed	25.90	26.57	27.81
Sample Size	1487	1487	1487

Table 3. Comparison statistics between collocated GOES-12 High Level (100-400mb) IR cloud-drift winds and rawinsondes over CONUS for the period April 25-30, 2003. Only winds whose height assignment was generated *from the CO2-IRW ratio algorithm* are included in this sample.

A comparison of the speed bias statistic between Tables 3 and 4, shows that the magnitude of the slow speed bias is largest when the CO_2 heights are selected. Given this, one might quickly suspect the problem is with the CO_2-IRW ratio algorithm. However, this is not the case. We determined that our decision method for choosing the final height assignment method, among the available height estimates, (i.e. H_20, CO_2 and IR window) was directly contributing to the observed slow speed bias. The tracer height selection method used in the current GOES high density winds processing system is very simplistic. Out of all the possible height assignments computed for each tracer, the one that is highest up in the atmosphere (i.e., the lowest pressure) is the one that is chosen. This approach worked well prior to GOES-12, when the H_2O-intercept and IR window methods were the only methods in use. With the introduction of the 13.3µm imager channel on board GOES-12, an additional height assignment method (CO_2-IRW ratio) is available for use to assign heights to high level tracers. Three viable height assignment methods (H_2O-intercept, CO_2-IRW ratio, and IR window), then, are available to assign a height to these high level tracers. Selecting the height that is highest up in the atmosphere may not be appropriate or desirable as it may not necessarily be the best one. This is especially true given that the mean characteristics of the water vapor intercept and CO_2 slicing heights are different. Our statistics show that for the same target scenes, the mean H_2O-intercept pressures tend to be lower than the corresponding CO_2 pressures by ~ 40mb.

Statistic	Satellite Wind	GFS model guess	Raob
Mean Vector Difference (m/s)	6.84	6.08	
Sat-Raob Speed Bias (m/s)	-1.66	-1.29	
Speed	24.20	24.55	25.84
Sample Size	1570	1570	1570

Table 4. Comparison statistics between collocated GOES-12 High Level (100-400mb) IR cloud-drift winds and rawinsondes over CONUS for the period April 25-30, 2003. Only winds whose height assignment was generated *from the water vapor intercept algorithm* are included in this sample.

This mean difference is consistent with the findings of Nieman et al, 1993 who showed mean differences between these two height assignments to be between 10-60mb on any given day. Schreiner et al, 2004 show that these mean differences can approach 100mb. These mean differences will influence the outcome of the tracer height selection method in a biased way. By virtue of the fact that the H_2O height is, in general, significantly higher up in the atmosphere than the corresponding CO_2 height, the H_2O-intercept height estimate will be selected more frequently than the CO_2 height estimate. Moreover, the sample of CO_2 heights that remain will exhibit a frequency distribution shifted towards lower pressure. The result is that the winds assigned CO_2 heights will appear to be, in the mean, too high in the atmosphere when compared against collocated rawinsonde winds. Consequently, these winds will exhibit a pronounced slow speed bias.

There are indications also that the H_2O-intercept estimates derived from G-12 data are being influenced by the broader spectral characteristics of that satellite's water vapor channel in such a way as to cause them to be assigned even higher in the atmosphere than corresponding H_2O-intercept estimates derived from G-8 and G-10 data. It is likely that these higher H_2O-intercept heights are further exacerbating the slow bias result by forcing the selection of still higher CO_2 height estimates. The results in Tables 3 and 4 appear to bear this out. Of course, the reverse situation, where H_2O-intercept heights are selected simply because they are higher up in the atmosphere, is also true, but to a lesser degree. Given the competing nature of the H_2O-intercept and CO_2 height assignments, the approach to select the one producing the height which is highest up in the atmosphere is not a desirable one. It is having a negative impact on the quality of the final wind products.

Several real-time parallel GOES-12 wind runs were setup. Table 5 describes the test runs and the satellite and rawinsonde comparison statistics for each of the runs. From these statistics, several conclusions can be drawn. First, the winds from the control run have the worst quality and possess the largest mean vector difference and the slowest speed bias. This is a reflection of the impact that selecting the height that is highest up in the atmosphere is having; namely, that the height selection method imposes a bias on the selected heights, placing them too high up in the atmosphere. Second, the quality of the GOES-12 winds is improved when the H_2O-intercept heights and CO_2 heights are not competing with each other. This result is reflected in the statistics for Test 1 (H_2O-intercept height only) and Test 2 (CO_2 heights only) where improvements over the control run in both the mean vector difference and speed bias are observed. Third, the quality of the GOES-12 winds is better when assigned CO_2 heights than when they are assigned H_2O-intercept heights. A comparison of the Test 1 and Test 2 results clearly indicates this. Based on this result, the height selection process has been modified in Test 3 to follow a pre-determined order. For each tracer, a CO_2 height is selected first (if available), then the H_2O-intercept height (if the CO_2 height is not available), and then the window height (if neither the CO_2 height nor the H_2O-intercept height are available). Inspection of the results from this test revealed significant improvements over the control run. The mean vector difference improved over the control run by 0.82 m/s and the speed bias was reduced from –1.84 m/s in the control run to –0.98 m/s in the test run. As a result of this analysis, the height selection process has been modified to follow a pre-determined order according to the expected performance of each height assignment algorithm. This approach resulted in significant improvements in the quality of the GOES-12 high level cloud-drift wind products.

Satwind - Raob Statistic	**Control** *H2O-int, CO2, & window heights; select lowest pressure*	**Test 1** *H2o-int & CO2 heights; select lowest pressure*	**Test 2** *CO2 & window heights; select lowest pressure*	**Test 3** *H2O-int, CO2 & window heights; select CO2 first, H2o-int, then window pressure*
Mean Vector Difference (m/s)	6.86	6.57	6.27	6.08
Sat-Raob Speed Bias (m/s)	-1.84	-1.54	-1.20	-0.98
Mean Sat/Raob Speed (m/s)	24.87/26.69	25.00/26.53	25.17/26.36	24.94/25.90
Sample Size	3220	2837	2712	2497

Table 5. Comparison statistics between collocated GOES-12 High Level (100-400mb) IR cloud-drift winds and rawinsondes over CONUS for the period April 25-30, 2003

2.4 MODIS winds

MODIS cloud-drift and water vapor wind observations from Terra and Aqua provide unprecedented coverage in the polar regions of the globe, areas where wind observations are sorely lacking. The capability to derive AMVs from MODIS measurements was first developed at CIMSS (Santek et al, 2004) and is based upon established methodologies and algorithms used to derive wind observations from the GOES series of satellites (Nieman et al., 1997). Key et al, 2004 describes how unique atmospheric and surface characteristics resident in the polar regions create challenges in assigning heights to tracers. Early model impact studies (Key et al, 2003; Bormann et al, 2004) showed that the MODIS winds had a positive impact on forecast accuracy, particularly over the polar regions.

Routine/experimental production of satellite winds from MODIS instruments aboard the Terra and Aqua satellites was established at NOAA/NESDIS in July 2003. The most significant modifications to the algorithms made by NOAA/NESDIS included targeting from the middle image in the image triplet and using the National Centers for Environmental Prediction (NCEP)'s global forecast model grids as the first guess in the MODIS winds processing scheme. Of these two changes, targeting from the middle image had the most significant impact on the MODIS AMVs and is, therefore, discussed below.

For GOES AMV processing, the middle image is used for target selection height assignment for all wind product types (Daniels et al, 2002). Winds vectors are computed forward and backward in time and averaged in this approach. This approach proved to be beneficial for GOES where a larger percentage of the targets selected resulted in good winds. For MODIS AMV processing, this approach proved to have significant positive impacts on the quality of the AMVs. This is illustrated in Table 6 which shows comparison statistics between mid-level (400-700mb) Terra cloud-drift winds and rawinsondes on June 2, 2004. Note the dramatic improvement in the mean vector difference and normalized RMS when the middle image targeting is used.

Statistic	**First Image Targeting**	**Middle Image Targeting**	**Raob**
Mean Vector Difference (m/s)	6.70	4.99	
Normalized RMS	0.42	0.30	
Sat-Raob Speed Bias (m/s)	-0.24	-0.53	
Speed	18.05	17.95	18.40
Sample Size	101	101	101

Table 6. Comparison statistics between collocated Terra Mid-Level (400-700mb) IR cloud-drift winds and rawinsondes over the Northern Hemisphere on June 2, 2004.

Middle image targeting appears to benefit the pattern recognition/feature tracking process. Its impact on the MODIS AMVs is greater than its impact on the GOES AMVs because of the much larger time interval between MODIS images. Targeting from the first image in a MODIS image triplet requires tracking of an identified feature over approximately 300 minutes (from the first image to the second image and then from the second image to the third image) during which time the identified feature can change shape through dissipation and evolution. Targeting from the middle image requires tracking the same identified feature over only about 100 minutes from the middle image to the first image (backward in time) and from the middle image to the third image (forward in time). There is evidence that this approach results in satellite winds which better resolve dynamic features. This is illustrated in Figure 3 which shows the relative vorticity fields derived from Terra AMVs where first image targeting was used (left) and where middle image targeting was used (right). Note the more pronounced vorticity maxima in the vorticity field for the middle image targeting case.

The changes made to the NOAA/NESDIS MODIS winds processing system were made in advance of the MODIS Winds Special Acquisition Period (MOWSAP) which occurred over the period November 5, 2003 – January 31, 2004. During this time period, both NOAA/NESDIS and CIMSS generated AMVs from Terra and Aqua and made them available to numerous Numerical Weather Prediction (NWP) centers for subsequent forecast model impact studies. NWP centers involved in assessing the MODIS winds during MOWSAP included: the Joint Center for Satellite Data Assimilation (JCSDA), European Center for Medium Range Weather Forecasting (ECMWF), United Kingdom Meteorological (UKMET) Office, Canadien Meteorological Center (CMC), the German Weather Service, and the NASA Global Modeling Assimilation Office (GMAO). All of these NWP centers (Cress, 2004; Kazumori et al, 2004, Forsythe, 2004, Riishojgaard et al, 2004, Sarrazin, 2004) showed positive impact on forecast skill in the polar region within their respective global forecast system.

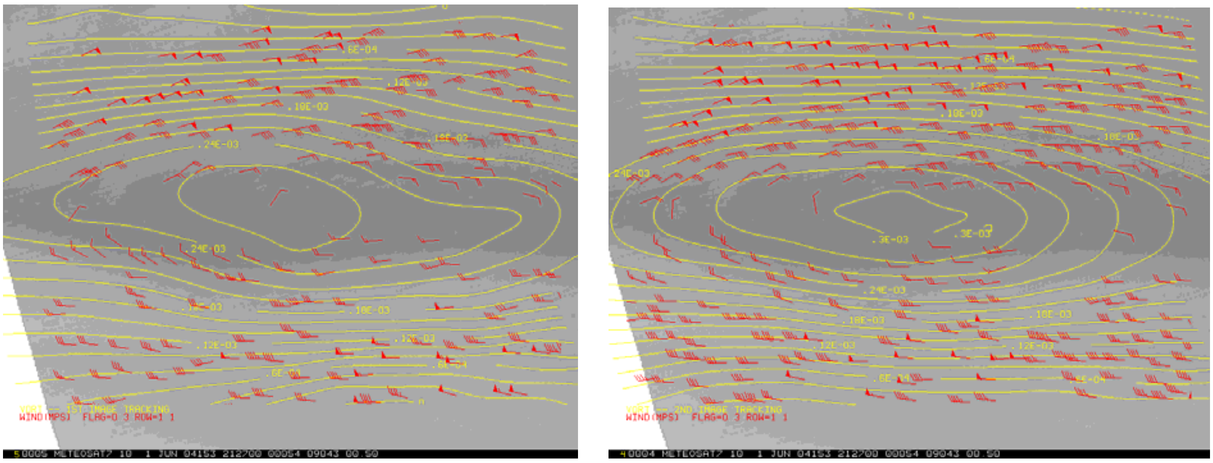

(a) (b)

Figure 3. Relative vorticity fields derived from Terra AMVs where first image targeting was used (a) and where middle image targeting was used (b).

NOAA/NESDIS is currently generating MODIS AMVs from Terra and Aqua on a routine basis and making them available on a ftp server (gp16.ssd.nesdis.noaa.gov) in the following directory (/pub/bufr/modis_winds). It is anticipated that these products will be distributed over the GTS beginning some time in late 2004.

3. RAPID SCAN WINDS

The utility of GOES rapid-scan winds continues to be demonstrated in field experiments designed to maximize observational abilities in regions of high-impact weather events. For example, the GOES rapid-scan WINDs EXperiment (GWINDEX) was again carried out for a two-month period in 2003 (Velden et al. 2001). The primary objective of GWINDEX is to demonstrate the improvement that could be gained in both quantity and quality of AMVs using GOES-10 RISOP imagery over the data-sparse northeast Pacific Ocean. The rapid-scan winds were produced in real time and provided mission-planning and forecast support to the coincident PACific landfalling JETs experiment (PACJET).

Special GOES Super Rapid Scan Operations (SRSO) periods have been collected during several Atlantic tropical cyclone (TC) events. The SRSO provides periods of continuous one-minute interval image sampling. Since TC cloud structures are characteristically fast-evolving, the advantages of super-rapid-scan imaging on AMV derivations can showcase a prime application. An example is illustrated in Figure 4 which shows low-level AMVs in the eye of Hurricane Isabel. These low level AMVs were derived using GOES-12 super-rapid-scan (3 minute intervals used) visible imagery. The ability to retrieve mesoscale cloud motions is notably enhanced using 3- to 5-minute image intervals. Regular use of the full 1-minute frequency is not practical, primarily due to intermittent navigation/registration inaccuracies introduced at this high-temporal imaging frequency. However, sophisticated image pre-processing and tracking methodology and high-end computers can help overcome these limitations (Hasler et al. 1998). Applications of these rapid-scan data sets extend to TC genesis studies, and research of TC intensity change (Knaff and Velden, 2000; Berger 2002).

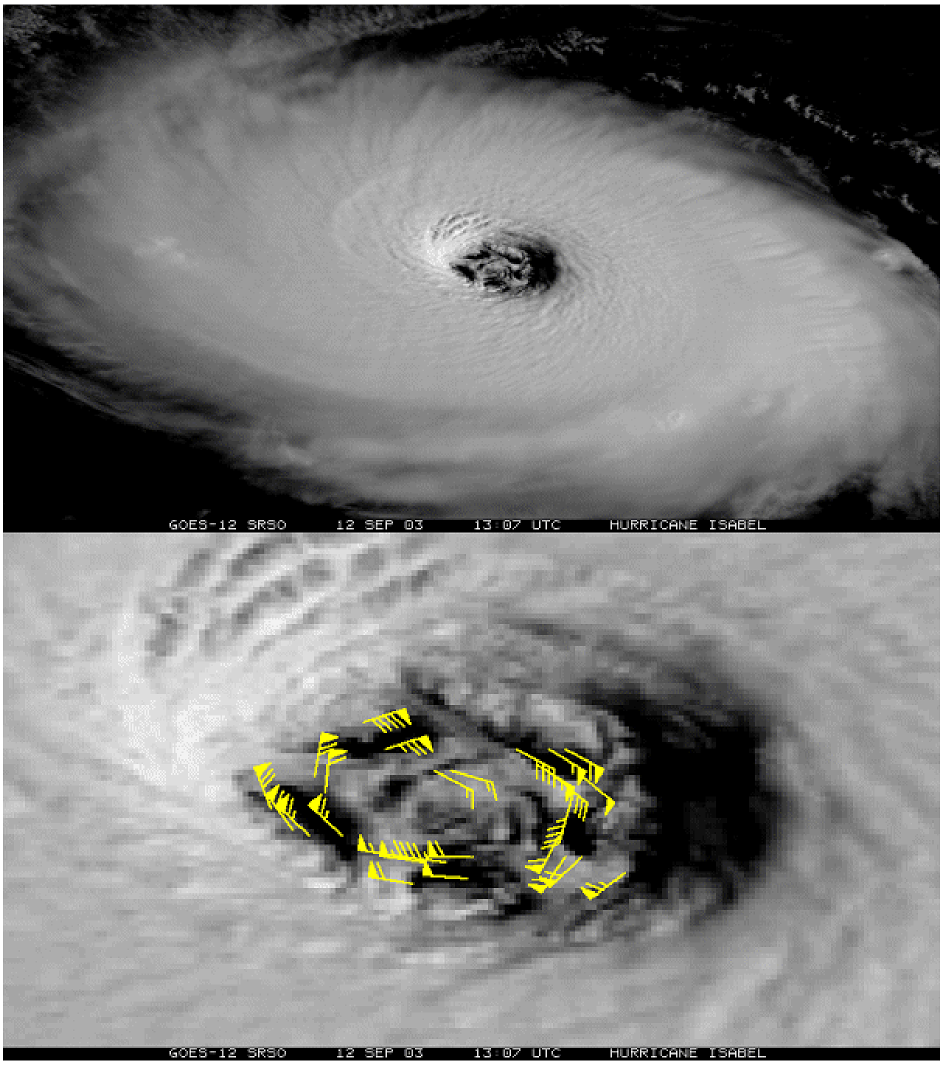

Figure 4. Hurricane Isabel in GOES-12 visible imagery on 12 September 2003 (top). Low-level AMVs in Isabel's eye derived from GOES-12 super-rapid scan (3-minute intervals used) visible imagery (bottom).

Other field programs are being designed to test "targeted" observations and adaptive sampling strategies. The concept of targeted observations is a focus of the newly formed THORPEX program, which is being developed under the auspices of the World Meteorological Organization (WMO) World Weather Research Program. The goal of this ten year international program is to accelerate improvements in the prediction of high impact weather on time scales out to two weeks. A new forecasting paradigm, that involves the development of a dynamically-interactive observing and forecast system, is envisioned. "Sensitive regions" will be identified and additional observations will be deployed there. Satellite observations will play a vital role in providing information on the atmospheric state in these regions. THORPEX will promote regional field campaigns and provide opportunities for creative adaptive sampling strategies. The most recent regional field campaign to occur was the Atlantic THORPEX REgional Campaign (A-TREC) which took place October 13-December 12, 2003. GOES-12 super rapid scan imagery and accompanying rapid scan winds, along with numerous other observational data types, were collected in "sensitive areas" over the Atlantic. GOES-12 super rapid scan wind products derived during this THORPEX A-TREC can be found at the following CIMSS web site: http://gale.ssec.wisc.edu/thorpex/thorpex.html.

4. HEIGHT ASSIGNMENT

4.1 Use of bias corrected radiances in the CO_2 slicing algorithm

For an infinitesimal cloud thickness at one pressure level, the difference in cloud-produced radiances, I(8), and corresponding clear air radiances, $I_{cl}(8)$, for a given field of view are written as:

$$I(8) - I_{cl}(8) = Zf \int_{Ps}^{Pc} \frac{9(8,p)\, dB[8,T(p)]\, dp}{dp}$$

where I (8) is the observed radiance, $I_{cl}(8)$ is the clear radiance at wavelength 8 and calculated from temperature and moisture profiles obtained from a short-term forecast from the NCEP global model, Zf is the effective cloud amount, P_s is surface pressure, P_c is cloud pressure, 9(8,p) is fractional transmittance for radiation of wavelength 8 emitted from the atmospheric pressure level (p) arriving at the top of the atmosphere (p=0), T(p) is the atmospheric temperature profile, B[8,T(p)] is the Planck radiance of wavelength 8 for temperature T(p). Given a priori knowledge of the temperature and moisture profile, satellite measurements of clear and cloudy radiances at a given wavelength leave one equation and two unknowns, Zf and P_c. With measurements at two wavelengths close enough together so that f_1 approximates f_2, the ratio of clear and cloudy sky radiance deviations in the two spectral wavelengths leaves an expression by which the cloud pressure within the field of view can be specified by:

$$\frac{I(8_2) - I_{cl}(8_2)}{I(8_1) - I_{cl}(8_1)} = \frac{\int_{Ps}^{Pc} 9(8_1,p)\, dB[8_1,T(p)]\, dp}{\int_{Ps}^{Pc} 9(8_2,p)\, dB[8_2,T(p)]\, dp}$$

The right side is calculated for a range of cloud top pressures, typically from 1000 – 100mb at 50mb intervals. The pressure where the left hand side equals the right hand side is the cloud top pressure.

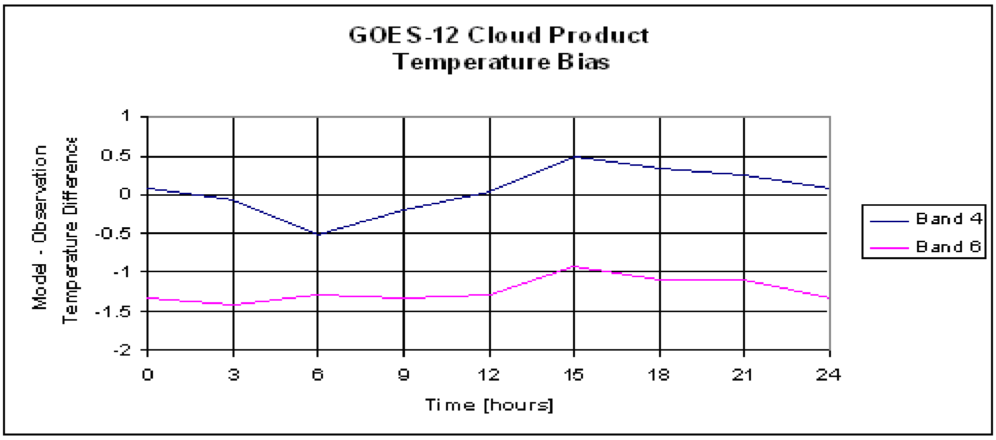

Figure 5. A 24 hour time series of the brightness temperature correction for GOES-12 imager band 4 (11.0µm) and band 6 (13.3µm)

Experiments were done that involved the application of a radiance bias correction to the CO_2 slicing algorithm. The radiance bias correction was computed for GOES-12 imager band 4 (11.0µm) and band 6 (13.3µm) using observed clear radiances over ocean and clear radiances computed using temperature and moisture profiles from NCEP's global model and the Pressure-Layer Optical Depth (PLOD) transmittance model, now commonly called the Pressure-layer Fast Algorithm for Atmospheric Transmittance (PFAAST) (Hannon, et al, 1996). Figure 5 shows a 24 hour time series of the brightness temperature bias correction for

GOES-12 imager band 4 and band 6. Note the diurnal variability evident in the bias corrections for both bands. Band 4 has largest diurnal variability while the magnitude of the bias correction is largest for band 6. The diurnal variability evident in the bias correction is likely due to both the satellite observations and the forecast model.

Table 7 shows the comparison statistics between GOES-12 high-level (100-400mb) cloud-drift winds, whose heights were assigned with CO_2 heights (with and without the bias correction) and rawinsondes. Note the drastic reduction in the mean vector difference and the speed bias. It is worth noting that the bias correction had the effect of moving the CO_2 heights downward in the atmosphere on the order of 50mb, which appears to be in the proper direction. These statistics indicate that a radiance bias correction should be applied.

Statistic	***Without* Radiance Bias Correction**	***With* Radiance Bias Correction**
Mean Vector Difference (m/s)	6.61	4.83
Normalized RMS	0.23	0.22
Sat-Raob Speed Bias (m/s)	–1.39	0.23
Speed (m/s)	26.85	26.40
Sample Size	853	853

Table 7. Comparison statistics between GOES-12 high-level (100-400mb) cloud-drift winds, whose heights were assigned with CO_2 heights (with and without the bias correction) and rawinsondes over the Northern Hemisphere from January 8-14, 2004.

4.2 A level of best-fit analysis

In an attempt to characterize heights assigned to AMV tracers, a level of best-analysis was performed using a year long (January – December 2002) database of collocated GOES-8 cloud-drift winds and rawinsonde wind profiles. The level of best-fit was defined to be the level at which the vector difference between the AMV and the rawinsonde wind is a minimum. Rao, et al., 2002 performed a similar analysis, but over a shorter period of time, and focused more on the clear-sky water vapor wind products. For each collocation record, a GOES-8 cloud-drift wind is compared to the entire rawinsonde wind profile resulting in a root mean square error (RMSE) vertical profile.

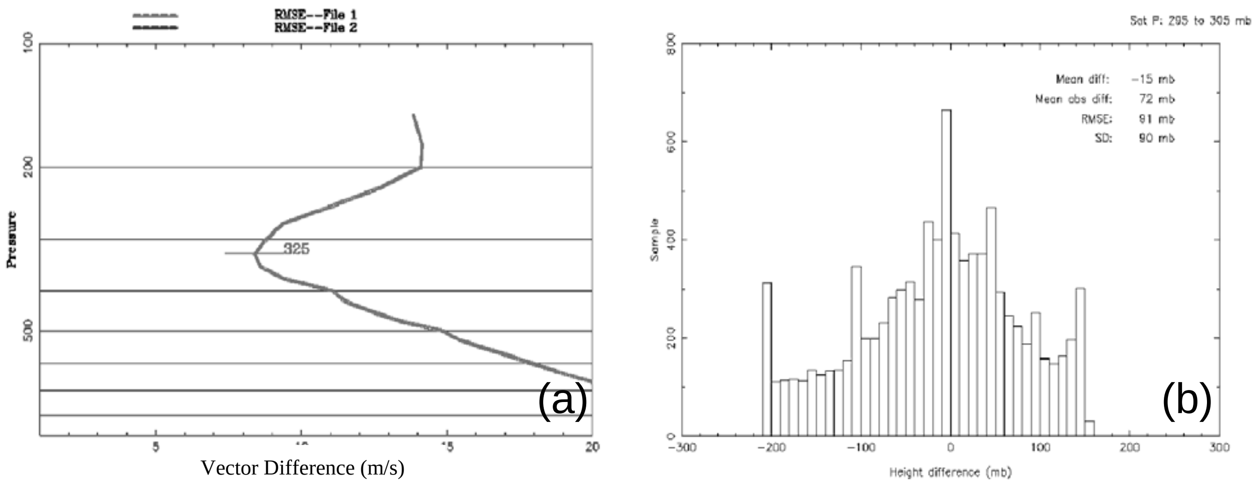

Figure 6. Vertical RMSE profile between GOES-8 cloud-drift winds at 300mb and entire rawinsonde profile (left) and histogram of individual height differences (pressure assigned to satellite wind – level of best-fit pressure) corresponding to vertical RMSE profile (right).

By doing this over the entire year period and stratifying the GOES-8 cloud-drift winds by height, yields a RMSE vertical profile like the one shown in Figure 6a which is for GOES-8 cloud-drift winds assigned at 300mb. Figure 6b shows the histogram of individual height differences (satellite winds at 300mb – level of best-fit pressure) corresponding to vertical RMSE profile in Figure 6a. It is important to note that the original height assignments (ie., before auto-editor height adjustments) were used in this analysis. Furthermore, the speed bias correction that is typically applied to the satellite winds at and above 300mb has been removed. A couple of observations can be made from Figures 6a and 6b. First, if the heights assigned to all of these GOES-8 winds were perfect, the minimum of the RMSE profile would occur at 300mb. As indicated in the figure, this is not the case. A slight height bias (satellite wind pressure – level of best fit pressure) of -25mb is indicated for the 300mb cloud-drift winds heights suggesting that as a whole, they are assigned too high up in the atmosphere. Second, the broadness of the profile about the minimum RMSE suggests that the satellite winds represent a layer rather than a single level. The corresponding histogram in Figure 6b is well behaved. It is Gaussian in nature, centered about zero, and has a standard deviation (about the mean value) of 90mb.

We extended this analysis to all GOES-8 wind types at numerous height assignment pressures. To do this, we stratified the GOES-8 winds by type (cloud-drift, cloud-top water, and clear-sky water vapor) and height (at every 25mb) and computed a RMSE profile and height difference histogram for these winds and plotted the height assignment bias as a function of height. The resulting vertical profiles of height bias for each wind type are shown in Figure 7. Error bars, indicating the standard deviation of the resulting height difference histograms, for the IR cloud-drift winds are plotted in this figure.

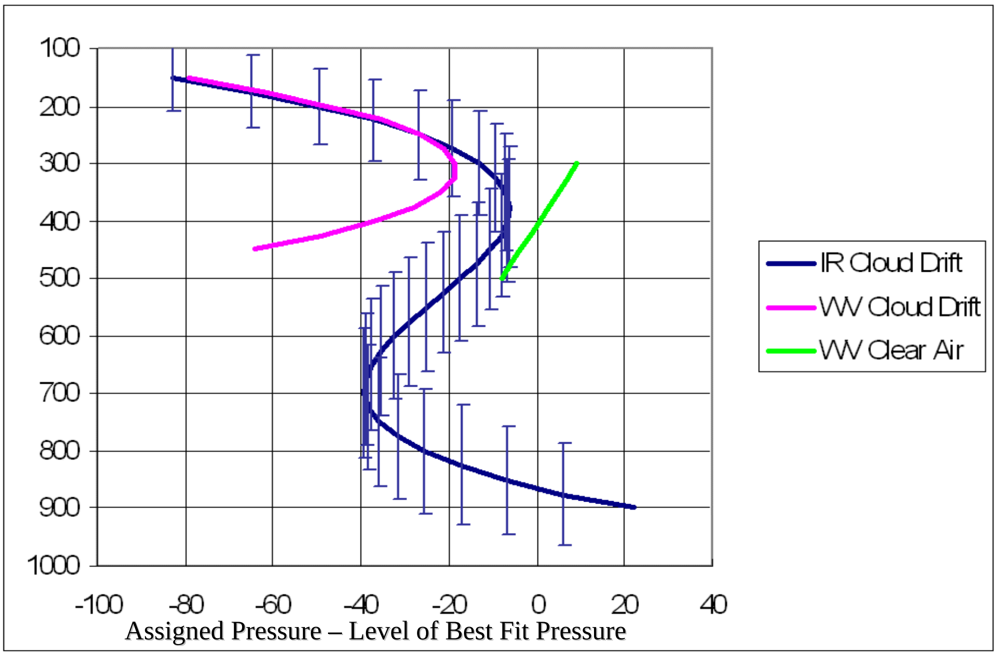

Figure 7. Height pressure difference (mb) profile (at every 25mb) between the assigned pressure and the level of best-fit pressure for GOES-8 IR cloud-drift, cloud-top water vapor, and clear-sky water vapor winds for the period Jan-Dec 2002. Error bars indicate one standard deviation about the mean difference values.

It is evident from this figure that, in the mean, the GOES-8 IR cloud-drift and cloud-top water vapour height assignments are assigned too high up in the atmosphere. The errors bars for the IR cloud-drift winds indicate that the histogram of the differences (assigned pressure – level of best-fit pressure) broadens as one moves downward in the atmosphere. The significance of this type of analysis is in the potential usefulness of the height bias and histogram broadness information to the NWP community who strive to optimize the assimilation of satellite derived winds in their NWP systems. This additional information may help set the vertical bounds for determining at which model layers these winds should be applied. These results also suggest there is room for improvement to the height assignment algorithms used in the current winds processing system. Further analysis of these data is planned where the data are stratified by height assignment method.

5. SUMMARY AND CONCLUSIONS

The status of the NOAA/NESDIS satellite wind product system has been discussed. GOES-12 replaced GOES-8 as the eastern operational geostationary satellite on May 1, 2003. The results of a detailed assessment of the GOES-12 AMVs, where the new 13.3µm channel was utilized to assign heights to cloud tracers, were presented. The addition of the 13.3µm channel has improved the quality of the high-level cloud-drift winds. Results presented in Section 4 highlighted the need to apply a radiance bias correction to the 13.3µm and 11µm channels prior to their use in the CO_2 slicing algorithm. This is not yet being done operationally as more work needs to be done. On May 22, 2003, GOES-9 was activated to provide coverage over the western Pacific for the international community until MTSAT-1R is launched and readied for operational service. The newest operational GOES AMV product is the low-level cloud-drift wind product derived from the 3.9µm channel. The GOES 3.9µm wind product is a night-time, low-level wind product that will complement the daytime, low-level visible cloud-drift wind product. Operational distribution of this product over the GTS is expected to begin in the Fall 2004. The utility of GOES rapid scan winds continues to be demonstrated in field experiments designed to maximize the observational abilities in regions of high-impact weather events. This will continue, particularly in light of the newly formed WMO THORPEX program that will promote numerous field campaigns requiring special targeted observations. The capability to generate AMVs over the polar regions from the MODIS instruments aboard the Terra and Aqua spacecrafts, has been added to the NOAA/NESDIS winds processing system. Many NWP centers have demonstrated that the MODIS winds have had an overwhelmingly positive impact on NWP forecast accuracy in the polar regions. NOAA/NESDIS plans to routinely generate MODIS AMVs and distribute them over the GTS in late 2004. Height assignment of AMVs continues to be an important issue. Results from a level of best-fit analysis involving GOES-8 AMVs were presented in Section 4 in an attempt to better characterize the height assignment errors associated with these AMVs. The results indicate the presence of a height bias for all wind types throughout a significant portion of the atmosphere. Information from this analysis may prove useful to NWP assimilation systems and to research efforts aimed at improving the quality of heights assigned to AMV tracers.

6. REFERENCES

Berger, H., 2002: The impact of GOES rapid-scan winds on ETA hurricane forecasts. Master’s Thesis, University of Wisconsin, 112 pp. Available from UW-AOS, 1225 W. Dayton St., Madison, WI 53706.

Bormann, Niels, Thépaut, Jean-Noël. 2004: Impact of MODIS Polar Winds in ECMWF's 4DVAR Data Assimilation System. *Monthly Weather Review*: Vol. 132, No. 4, pp. 929–940.

Cress, A., 2004: Impact of MODIS winds in the global NWP system of the German Weather Service. *Proceedings of the 7th IWW*, Helsinki, Finland, these proceedings.

Daniels, J., C. Velden, W. Bresky, A. Irving and K. Turner, 2002: Status and development of GOES wind products at NOAA/NESDIS. *Proceedings of the 6th IWW*, Madison, WI, 71-80. Copies available from EUMETSAT, Am Kavalleriesand 31, D-64295, Darmstadt, Germany.

Dunion, J.P., and C.S. Velden, 2002a: Using the GOES 3.9 micron shortwave channel to track low-level cloud-drift winds. *Proceedings of the 6th IWW*, Madison, WI, 277-282. Copies available from EUMETSAT, Am Kavalleriesand 31, D-64295, Darmstadt, Germany.

Forsythe, M., 2004: MODIS winds: Latest results at the MET Office. *Proceedings of the 7th IWW*, Helsinki, Finland, these proceedings.

Hannon, S., L. Strow, and W. McMillan, 1996: Optical spectroscopic techniques and instrumentation for atmospheric and space research II. Proceedings of SPIE conference, pg. 2830.

Hasler, A.F., et al., 1998: High-resolution wind fields within the inner core and eye of a mature tropical cyclone from GOES 1-min. images*. Bull. Amer. Meteor. Soc*., 79, 2483-2496

Kazumori, M and Y. Nakamura, 2004: MODIS polar winds assimilation experiments at JMA. *Proceedings of the 7th IWW*, Helsinki, Finland, these proceedings.

Key, J., D. Santek, C.S. Velden, N. Bormann, J.-N. Thepaut, L.P. Riishojgaard, Y. Zhu, and W.P. Menzel, 2003, Cloud-drift and Water Vapor Winds in the Polar Regions from MODIS. *IEEE Trans. Geosci. Remote Sensing*, 41(2), 482-492.

Key, J., D. Santek, and C. Velden, 2004: Atmospheric motion vector height assignment in the polar regions: issues, and recommendations. *Proceedings of the 7th IWW*, Helsinki, Finland, these proceedings.

Knaff, J. and C. Velden, 2000: Relationships between the multi-layered wind field and the intensity of Hurricane Floyd. 24th AMS Conf. Hurricanes and Trop. Meteor., Ft. Lauderdale, FL, 492-493.

LeMarshall, J., G. Mills, R. Seecamp, N. Pescod, L. Leslie and A. Rea, 2002: High density AMVs and their application to operational NWP. *Proceedings of the 6th IWW*, Madison, WI, 137-146. Copies available from EUMETSAT, Am Kavalleriesand 31, D-64295, Darmstadt, Germany.

Menzel, W.P., W.L. Smith, T.R. Stewart, 1983: Improved cloud motion wind vector and altitude height assignment using VAS. *J. Clim. Appl. Meteor*., 22, 377-384.

Nieman, S., J. Schmetz and P. Menzel, 1993: A comparison of several techniques to assign heights to cloud tracers. *J. Appl. Meteor*., 32, 1559-1568.

Rao, A., C. Velden and S. Braun, 2002: The vertical error characteristics of GOES-derived winds: Description and experiments with NWP. *J. Appl. Meteor.*, 41, 253-271.

Riishojgaard, L. and Y. Zhu, 2004: Impact experiments on GMAO data assimilation and forecast systems with MODIS winds during MOWSAP. *Proceedings of the 7th IWW*, Helsinki, Finland, these proceedings.

Sarrazin, R., 2004: MODIS polar winds assimilation impact study with CMC operational NWP system. *Proceedings of the 7th IWW*, Helsinki, Finland, these proceedings.

Schreiner, A.J., W.P. Menzel, A. Heidinger, J. Davies, and W. Feltz, 2004: Comparisons of cloud motion vector height assignment techniques using the GOES-12 imager. *Proceedings of the 7th IWW*, Helsinki, Finland, these proceedings.

Santek, D., C. Velden, and J. Key, 2004: Polar winds from MODIS: Project Status. *Proceedings of the 7th IWW*, Helsinki, Finland, these proceedings.

Szejwach, Gerard. 1982: Determination of Semi-Transparent Cirrus Cloud Temperature from Infrared Radiances: Application to METEOSAT. *Journal of Applied Meteorology*: Vol. 21, No. 3, pp. 384–393.

Velden, C., D. Stettner, J. Daniels and W. Bresky, 2001: GWINDEX: Applications for west coast forecasting. *11th AMS Conf. on Satellite Meteor*., Madison, WI, 244-247.